A METHOD FOR THE ANALYSIS OF HIGH POWER BATTERY DESIGNS

Andrew F. Burke
Institute of Transportation Studies
University of California, Davis
Davis, California 95616
Phone (916) 752-9812 Fax (916) 752-6572

ABSTRACT

A spreadsheet model for the analysis of batteries of various types has been developed that permits the calculation of the size and performance characteristics of the battery based on its internal geometry and electrode/electrolyte material properties. The method accounts for most of the electrochemical mechanisms in both the anode and cathode without solving the governing partial differential equations. The spreadsheet calculations for a particular battery design are performed much like a battery test in that the C/3 capacity of the battery to a specified cut-off voltage is determined and then the pulse power capability at a given state-of-charge is determined by finding the maximum current density (A/cm2) for which the cell voltage equals a specified minimum value. For a multi-cell module, the module characteristics are calculated using the cell results and packaging input information. The spreadsheet model has been validated for existing lead-acid (Sonnenschein), nickel cadmium (Saft), and nickel metal hydride (Ovonic) batteries for which test data and internal geometry information are available. Various battery designs were then evaluated using the method to show how batteries having high power densities (greater than 500 W/kg) could be designed. The spreadsheet model permitted the determination of the critical design parameters for high power lead-acid, nickel cadmium, and nickel metal hydride batteries.

INTRODUCTION

The primary objective of this work was to develop a method for the analysis of batteries of various types that could be used as a tool to link battery design, performance, especially peak power density and energy density, and cost. There are numerous papers (References 1-5) in the literature that model batteries in great detail starting with the governing partial differential equations that are solved in space, usually in one dimension, and time to determine the concentration and ion current distributions between the electrodes of the battery. These analyzes are valuable for understanding why batteries of a particular design behave as they do, but are cumbersome to use as a design tool to study the effect of battery geometry and material parameters on performance and life cycle and cost related characteristics, such as electrode thickness and area. It was also desired that the method be relatively easily adapted to the analysis of different battery types. One of the motivations for this work was to have a means of analyzing the trade-offs between energy density and peak power density as such trade-offs are often claimed as one of the reasons for using ultracapacitors to load level batteries in electric vehicles.

In order to meet these objectives, it was necessary that the method developed describe the configuration and materials in the cell/module in detail and include the principal electrochemical mechanisms that effect the voltage drop and current flow in the battery. In developing the general, but relatively simple, model of the battery discussed in this paper, the works presented in great detail in References (1-6) were invaluable as sources of electrode material and electrolyte properties and discussions of the basic governing equations. Second sources of valuable information were various battery test reports, especially those from the Idaho National Engineering Laboratory (References 7-8) that showed the discharge characteristics of several type of batteries and the battery internal design parameters based on post-test tear-down studies. This information was invaluable in determining input data for the present calculations and permitting the validation of the method developed for specific battery designs. Validation was done in terms of comparing calculated and measured values for Ah capacity and energy density for constant current discharges, peak power density for a specified voltage cutoff, cell resistance, and module weight and dimensions

GENERAL APPROACH

The intent was to develop battery models using spreadsheet software (EXCEL) that described the essence of the electrochemical mechanisms in the battery without solving the governing partial differential equations. It was also desired that the model could be exercised to determine the performance characteristics of a particular battery design in much the same way that a battery would be tested - that is discharged at constant current to a specified cut-off voltage and then discharged at high currents for short pulses to determine its peak power density and resistance. These objectives were met in the following way. Battery state-of-charge, given in terms of active material utilization, was used in place of discharge time. Useable Ah capacity for a specified current density (A/cm2) was determined by varying the material utilization fraction at that current until the voltage at that utilization fraction equaled the specified cut-off voltage. The maximum current density (A/cm2) and thus the peak power density at a specified depth-of-discharge for a particular battery design was found by varying the current density until the calculated voltage at that state-of-charge (material utilization fraction) equaled the specified cut-off voltage for short pulses. Hence running the spreadsheet is much like testing a battery in that one varies the current (A/cm2) and observes the resultant voltage behavior of the battery.

The battery cell is described in terms of its component parts: (1) anode, (2) cathode, and (3) separator/electrolyte (see Figure 1). Each of the parts is prescribed in terms of its geometry (thickness) and material properties (chemistry, porosity, surface area, density, specific resistance, etc.). The anode and cathode are made up of a current collector or grid and an active electrode layer. The characteristics of the grid and active layer are specified individually. The chemistries of the anode and cathode materials are given in terms of the molecular weight, charge number, and Ah/gm of the active materials and products and the standard potentials and reference exchange currents needed to describe the Tafel equation for the electrode surface interfaces. Provision is made for inert binders in the electrode layers. The separator is specified in terms of its thickness, porosity, and specific resistance. The electrolyte is described in terms of its density, ionic resistivity, diffusion coefficient, and transference number. The voltage changes in the anode, cathode, and separator are calculated separately for the specified current density and active material utilization fraction, which are inputs to each trial calculation of the spreadsheet. The voltage changes across each part of the cell include the effect of changes in the ion concentration in the electrolyte and the active material availability at the electrode surfaces on the electrode open circuit potentials and exchange currents as the battery discharges. Average concentration and voltage gradients are calculated for each electrode from the required ion fluxes at the specified current density (A/cm2). The concentration and voltage changes are then calculated from the product of the average gradient and mean electrode thickness. After the cell characteristics are determined on a unit area (cm2) basis, the area required in an actual cell to meet the specified Ah capacity is calculated. The weight and size of the various component parts of the cell are then determined and the energy density and peak power density calculated. The output of the spreadsheet yields a complete description of the cell and its performance. The final step in the calculation is to combine the cells into a module of a prescribed voltage and to calculate the characteristics of the module.

This general approach has been applied to lead-acid, nickel cadmium, and nickel metal hydride batteries. Input data for those battery types and selected results from the spreadsheet calculations are discussed in the next section.

APPLICATION OF THE METHOD TO SPECIFIC BATTERY TYPES AND DESIGNS

Validation of the Method

This approach to battery analysis has been validated by applying it to several existing batteries for which there were test data and reasonable knowledge of the battery internal construction and materials characteristics. The batteries selected were the Sonnenschein DF 6V-160 sealed lead-acid battery (Reference 8), the SAFT SEH-5-200 nickel cadmium battery (Reference 9), and the Ovonic 14V-90Ah nickel metal hydride battery (References 9-10). Each of these batteries was analyzed using the spreadsheet model. In each case, the battery positive and negative plates were sized to yield the measured C/3 Ah capacity. When information on thicknesses of the grids and active layers of the electrode plates were available, it was used in setting up the inputs for the analysis of the battery. As shown in Tables 1 and 2, which are listings of the inputs for the Sonnenschein and Ovonic batteries, the batteries are described in considerable detail in terms of their construction, materials, and electrochemical characteristics. For the three batteries being analyzed, some of the input quantities were known with relatively little uncertainty while there was considerable uncertainty for some of the input parameters. In the latter instances, the input parameters were varied over physically appropriate ranges and values were determined that yielded a set of battery cell/module characteristics that were consistent with the known weight, dimensions, and performance of the battery. As shown in Table 3, the spreadsheet model yielded results in good agreement with the actual/measured characteristics of the three batteries being analyzed. No attempt was made to refine the inputs for each battery to bring the overall agreement between the calculated and measured values to better than about 10%, because of the large number of inputs involved. In future work, it is planned to contact the battery manufacturers directly and attempt to get from them actual values of dimensions and material properties for their batteries. Nevertheless, the good agreement shown in Table 3 indicates the general validity of the approach for battery analysis and justifies the application of the method to assess the performance of advanced battery designs.

Application to Various Battery Designs

Lead-acid batteries.

The method has been applied to a series of lead-acid battery designs as shown in Table 4. The thicknesses of the grids/current collectors, plates, and separator have been varied over wide ranges. The Ah capacity of the cells has also been varied. The results shown in Table 4 indicate that it should be possible to design lead-acid batteries having very high power density with a relatively small sacrifice in energy density. This requires that the current collectors and plates be very

thin compared with thicknesses used in most existing batteries. The results for the small 1.2 Ah design, which is intended to represent that of the Bolder Technologies battery, shows performance close to that reported in Reference (11) for that battery/cell. For the lead-acid batteries, the separator thickness and grid openness are particularly critical parameters. The results indicate that a high power, high energy density lead-acid battery should utilize a current collector with large openness and distributed current collecting capability, like a foam. A thin foil, like that used in the Bolder Technology battery yielded high power density, but lower energy density. Thin plates in the lead-acid batteries seem to result in significantly higher active material utilization than is achieved in thicker plate batteries, such as the Sonnenschein DF 6V-160. A key factor that is not addressed in the present work is the effect of the thin plates on battery cycle life. If, as seems likely, achieving long cycle life with the very high power density designs is difficult or nearly impossible, the primary advantage of using ultracapacitors to load level the "energy" battery in an electric vehicle will be to extend its cycle life. The high power density batteries also have high plate area per Ah and thus high cost.

Nickel cadmium batteries.

A series of nickel cadmium battery designs were also evaluated using the spreadsheet model. The results shown in Table 5 indicate that high power density (W/kg) can be achieved with nickel cadmium batteries. As with lead-acid batteries, high power density requires thin plates. However, unlike lead-acid batteries, the power density in nickel cadmium batteries is much less sensitive to current collector openness and separator thickness. It does not seem possible to achieve the very high power densities of 2000 W/kg and greater than is the case for the thin film lead-acid batteries. Also the results in Table 5 indicate that achieving high power in nickel cadmium batteries will require a sacrifice in energy density. However, it seems likely that it will be less difficult to achieve high cycle life with thin plate nickel cadmium batteries than with thin plate lead-acid batteries.

Nickel metal hydride batteries.

Nickel metal hydride batteries designs were also evaluated using the spreadsheet model. The results of the calculations are shown in Table 6. The Ah capacity of the cells was varied from 90 to 5 Ah for plate thicknesses between .008 and .06 cm. The critical material parameters for this battery are the percent hydrogen storage and particle radius of the hydride material in the anode. The spreadsheet results indicate that high power density (800-900 W/kg) nickel metal hydride cells can be designed using thin plates and anode material having a 2% hydrogen storage capacity and a small particle radius of 20 microns. High power density can be achieved using either foil type or foamed open sheet electrodes, but it appears that using thin foil as the current collector results in an energy density penalty compared with the open electrodes. As in the case of the other battery types, a primary consideration for the nickel metal hydride batteries is the cycle life of the thin film batteries needed to achieve power densities of 500-1000 W/kg.

REFERENCES

1. Bernardi, D. and Carpenter, M.K., A Mathematical Model of the Oxygen-Recombination Lead-acid Cell, J. Electrochemical Society, Vol. 142, No.8, August 1955
2. Fan, D. and White, R.E., A Mathematical Model of a Sealed Nickel-Cadmium Battery, J. Electrochemical Society, Vol. 138, No.1, January 1991
3. Mao, Z., DeVidts, P., White, R.E., and Newman,J., Theoretical Analysis of the Discharge of a NiOOH/H2 Cell, J. Electrochemical Society, Vol. 141, No.1, January 1994
4. Bernardi, D.W., Hiram, G., and Schoene, A.Y., Two-Dimensional Mathematical Model of a Lead-Acid Cell, J. Electrochemical Society, Vol. 140, No.8, August 1993
5. Fan, D. and White, R.E., Mathematical Modeling of a Nickel-Cadmium Battery (Effects of Intercalation and Oxygen Reactions), J. Electrochemical Society, Vol.138, No.10, October 1991
6. Newman, J.S., Electrochemical Systems (Second Edition), Prentice Hall, Inc. , 1991
7. Hardin, J.E., Laboratory Testing and Post-Test Analysis of the Sonnenschein DF-6V-160 6-Volt Traction Battery, EG&G Report EGG-EP-10746, May 1993
8. Hardin, J.E., Laboratory Testing of the SAFT SEH-5-200 6 Volt Traction Battery, EG&G Report EGG-EP-8917, December 1989
9. Delco Ovonic Battery brochure and private communications with D.A. Corrigan
10. Ovshinsky, S.R., and etals, Ovonic NiMH Battery Technology for Portable and Electric Vehicle Applications, Paper presented at the Thirteenth International Seminar on Primary and Secondary Battery Technology and Applications, Deerfield Beach, Florida, March 1996
11. Keating, J., Schroeder, and Nelson, R., Development of a Valve-Regulated Lead-acid Battery Power-Assist Hybrid Electric Vehicle Use, Bolder Technologies Corp.

Figure 1: Cell Geometry

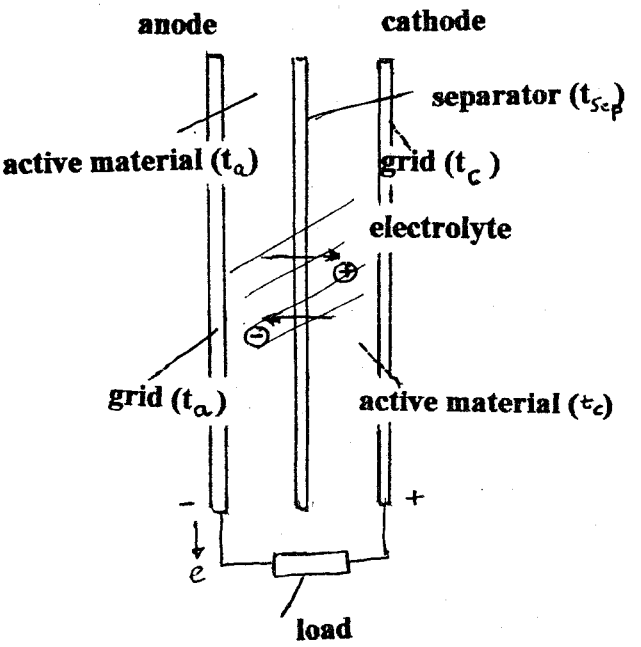

Table 1: Model Inputs for Lead-Acid Batteries

138	Ah	3	cells/module
Anode (negative plate of spongy Pb)			
Grid (current collector)			
	Density (gm/cm3)		11.3
	resistance (ohm-cm2)		0.00072
	Thickness (cm)		0.0975
	openness (%)		70
Active material (after formation)			
	Density (gm/cm3)		11.3
	PbSo4 density (gm/cm3)		6.3
	Thickness (cm)		0.15
	Initial porosity (100*%)		0.75
	Surface area (cm2/cm3)		2.50E+04
	theoretical Capacity (Ah/gm)		0.259
	specific resistance (ohm-cm)		2.00E-05
	Standard potential (Volts)		0.344
	Reference exchange current (A/cm2)		8.00E-06
	Reference concentration (moles/liter)		4.9
	Torquosity factor		1.5
	Molecular weight (gm-mole)		207
	grid thickness/plate thickness		0.65
	transfer coefficient		0.5
cathode (positive plate of PbO2)			
Grid (current collector)			
	density (gm/cm3)		11.3
	resistance (ohm-cm2)		0.00072
	Thickness (cm)		0.108
	openness (%)		70
Active material			
	density (gm/cm3)		9.7
	PbSo4 density (gm/cm3)		6.3
	Thickness (cm)		0.167
	Initial Porosity		0.7
	Surface area (cm2/cm3)		2.50E+05
	theoretical capacity (Ah/gm)		0.224
	specific resistance (ohm-cm)		2.00E-05
	Standard potential (volts)		1.6282
	Reference exchange current (A/cm2)		6.00E-07
	Reference concentration (moles/liter)		4.9
	Torquosity factor		1.5
	Molecular weight		239
	grid thickness/plate thickness		0.65
	transfer coefficient		0.5
Separator			
	density (gm/cm3)		0.05
	thickness (cm)		0.194
	porosity		0.8
	specific resistance (ohm-cm)		0.001
electrolyte (sulfuric acid)			
	initial density (gm/cm3)		1.258
	solvent/ions water H SO4-, H+		
	ionic resistivity (Ohm-cm)		0.5
	reference ion concentration (moles/liter)		4.9
	reference diffusion coefficient (cm2/sec)		2.00E-05
	Postive ion transference number		0.72
	initial ion concentration (moles/cm3)		4.90E-03
Condition of the discharge			
	set type of discharge flgdc3=3 (C/3), flgdc3=1,mx power		
	Temperature (deg Kelvin)		300
	estimated state-of-charge		0.6
	cutoff-voltage/cell		1.75
	minimum voltage/cell at high power		1.33
	estimated current density at C/3 (A/cm2)		0.012
	estimated max current density (A/cm2)		0.172
	nominal cell voltage		2
	material utilization at C/3 discharge		0.4
module parameters			
	plate height(cm)		19
	plate width (cm)		16
	container thickness (cm)		0.185
	cell divider thickness (cm)		0.2
	container density (gm/cm3)		1
	terminal diameter (cm)		1.9
	terminal height (cm)		1.9
	ratio intercell/plate connector/grid weight		1.4

Table 2: Model Inputs for Nickel Metal Hydride Batteries

88	Ah	1	cells/module
Anode (negative plate of metal hydride)			
Grid (current collector-nickel screen)			
	Density (gm/cm3)		8.8
	resistance (ohm-cm)		0.00075
	Thickness (cm)		0.005
	openness (%)		90
Active material (after formation)			
	Density (gm/cm3)		5.69
	density (gm/cm3) of hydride after discharge		5.69
	Thickness (cm)		0.016
	Initial porosity (100*%)		0.6
	Surface area (cm2/cm3)		2.00E+03
	theoretical Capacity (Ah/gm)		0.268 Ah/g
	specific resistance (ohm-cm)		2.00E-05
	Standard potential (Volts)		-.08
	Reference exchange current (A/cm2)		2.84E-04
	Reference concentration (moles/liter)		6 OH-
	Torquosity factor		1.5
	Molecular weight (gm-mole)		50
	grid thickness/plate thickness		0.33
	transfer coefficient		0.5
	hydride particle radius (cm)		0.003
	hydride diffusion coefficient (cm2/sec)		5.00E-10
	percent hydrogen storage in hydride		2
	initial H concentration (moles H/cm3)		0.1138
	number of terms in diffusion solution		20
	order of reaction for H		0.67
	theoretical capacity (Ah/gm) -specified %H		0.536
cathode (positive plate of NOOH on foamed nickel)			
Grid (current collector)			
	density (gm/cm3)		8.8
	resistance (ohm-cm2)		0.00072
	Thickness (cm)		0.03
	openness (%)		90
Active material			
	density (gm/cm3)		5.826772
	Ni(OH)2 density (gm/cm3)		4.83
	Thickness (cm)		0.045
	Initial Porosity (%)		0.65
	Surface area (cm2/cm3)		4.00E+03
	theoretical capacity (Ah/gm)		0.291
	specific resistance (ohm-cm)		2.00E-05
	Standard potential (volts)		0.45
	Reference exchange current (A/cm2)		6.10E-05
	Reference concentration (moles/liter)		7.1
	Torquosity factor		1.5
	Molecular weight		92
	grid thickness/plate thickness		0.9
	transfer coefficient		0.5
Separator			
	density (gm/cm3)		0.1
	thickness (cm)		0.075
	porosity		0.8
	specific resistance (ohm-cm)		0.08
electrolyte (KOH)			
	initial density (gm/cm3)		1.245
	solvent/ions water OH-, H+		
	ionic resistivity (Ohm-cm)		1.87
	reference ion concentration (moles/liter)		7.1
	reference diffusion coefficient (cm2/sec)		2.57E-05
	Postive ion transference number		0.78
	initial ion concentration (moles/cm3)		5.00E-03
conditions for the discharge			
set type of discharge flgdc=3 (C/3), flgdc3=1, max power			
	Temperature (deg Kelvin)		300
	estimated state-of-charge		0.06
	cutoff-voltage/cell		1
	minimum voltage/cell at high power		0.8
	estimated current density at C/3 (A/cm2)		0.064
	estimated max current density (A/cm2)		0.12
	nominal cell voltage		1.3
	material utilization at C/3 discharge		0.94
module parameters			
	plate height(cm)		15
	plate width (cm)		8.5
	container thickness (cm)		0.02
	cell divider thickness (cm)		0.0001
	stainless steel container density (gm/cm3)		7.75
	terminal radius (cm)		0.3
	terminal height (cm)		1
	ratio intercell/plate connector/grid weight		2

TABLE 3: VALIDATION RE SULTS FOR THREE BATTERY TYPES

Sealed Lead-Acid Battery Sonnenschein DF-6V-160		
	Actual	Model
c/3 Capacity (Ah)	138	138
Weight (kg)	32.4	32.8
(wh/kg) c/3	25	25.2
Length (cm)	25.9	22.7
No. of Plates	15-16	15
(w/kg) max at 75% DOD	160	192
Resistance (ohms)	.00064/cell	.00086/cell

Nickel Cadmium Battery SAFT SEH-5-200		
	Actual	Model
c/3 Capacity (Ah)	204	204
Weight/(kg)	24.9	22.7
(wh/kg)c/3	55.0	49.9
Length (cm)	24.5	28.0
No. of Plates	15-16	15
(w/kg) max at 75% DOD	160	192
Resistance (ohms)	.00042/cell	.000433/cell

Nickel Metal Hydride Ovonic 1.3V, 90 Ah		
	Actual	Model
c/3 Capacity (Ah)	90	90
Weight (kg)	1.62	1.8
(Wh/kg)c/3	70	63
Length (cm)	3.7	3.4
No. of Plates	-	17
(W/kg)max at 75% DOD	>220	278
Resistance (Λ)	.00105/cell	.0007/cell

TABLE 4: MODELING RESULTS FOR VARIOUS DESIGNS OF SEALED LEAD-ACID BATTERIES

	Grid		Anode		Cathode		Separator	Cell/Module			
(Ah)c/3	th (cm)	% open	th (cm)	porosity	th (cm)	porosity	th (cm)	Ah cm^2	Wh/kg) c/3	(W/kg)max 70% DOD	area cm^{2}cell
138,12V	.0975	70	.15	.75	.167	.7	.105	.0347	25.2	93	3975
50,12V	.04	80	.05	.70	.06	.7	.075	.0168	46.9	364	2975
50,12V	.01	80	.03	.70	.03	.7	.05	.0100	55.3	1492	4977
50,12V	.005	0	.02	.70	.025	.7	.03	.0068	37.5	1583	7375
1.2,2V	.0025	0	.0125	.70	.0125	.7	.015	.0037	26.1	2880	323

TABLE 5: MODELING RESULTS FOR VARIOUS DESIGNS OF NICKEL CADMIUM BATTERIES

	Grid/Foam		Anode		Separator	Cathode		Cell/module			
(Ah)c/3	th (cm)	% open	th (cm)	porosity	th (cm)	th (cm)	porosity	ah/cm^2	(Wh/kg)c/3	(Wh/kg)mg	area cm^2/cell
204,6V	.004	10	.044	.67	.1	.050	.6	.038	69	183	5337
204,6V	.004	10	.060	.67	.1	.080	.6	.038	69	183	5337
50,6V	.008	90	.010	.5	.075	.012	.4	.008	45	490	6263
10,6V	.005	90	.007	.6	.025	.008	.4	.0054	47	576	1854

TABLE 6: MODELING RESULTS FOR VARIOUS DESIGNS OF NICKEL METAL HYDRIDE BATTERIES

	Grid		Anode				Cathode		Module/Cell			
(Ah)c/3	th (cm)	% open	th (cm)	porosity	rp(u)	% H_2	th (cm)	porosity	Ah/cm^2	(Wh/kg)c/ 3	(W/kg)max 70% DOD	area cm^2/cell
90,1.3V	.012	92	.045	.6	30	1.25	.06	.5	.033	6	301	2734
90,1.3V	.012	92	.045	.6	20	1.75	.06	.5	.046	8	440	1953
90,1.3V	.005	92	.015	.6	30	1.75	.045	.65	.016	61	300	5524
90,1.3V	.005	92	.015	.6	20	2.0	.045	.70	.0186	71	443	4833
10,1.3V	.0025	0	.0125	.70	20	2.0	.0125	.70	.0045	37	834	2228
5,1.3V	.005	90	.008	.70	20	2.0	.009	.70	.0038	60	905	1311